

Risk Controlled Image Retrieval

Kaiwen Cai, Chris Xiaoxuan Lu, Xingyu Zhao, Xiaowei Huang

Abstract

Most image retrieval research focuses on improving predictive performance, but they may fall short in scenarios where the reliability of the prediction is crucial. Though uncertainty quantification can help by assessing uncertainty for query and database images, this method can provide only a heuristic estimate rather than a *guarantee*. To address these limitations, we present Risk Controlled Image Retrieval (RCIR), which generates retrieval sets that are guaranteed to contain the ground truth samples with a predefined probability. RCIR can be easily plugged into any image retrieval method, agnostic to data distribution and model selection. To the best of our knowledge, this is the first work that provides coverage guarantees for image retrieval. The validity and efficiency of RCIR is demonstrated on four real-world image retrieval datasets, including the Stanford CAR-196 (Krause et al. 2013), CUB-200 (Wah et al. 2011), the Pittsburgh dataset (Torii et al. 2013) and the ChestX-Det dataset (Lian et al. 2021).

1 Introduction

Given a query image, the goal of an image retrieval system is to find the best matching candidates from the database. Image retrieval has long been studied and has paved the foundation for many computer vision applications, including face recognition (Cheng and Wang 2019), large scale image classification (Warburg et al. 2021) and person re-identification (Yao et al. 2019).

Image retrieval works by representing each image as a vector in a high dimensional space and finding the nearest neighbors of the query image in the database. Discriminative image representations are crucial for this process. Massive research has been devoted to improving the representation power of image features, spanning from early hand-crafted features to nowadays deep learning based ones. However, like any deep learning based methods, current image retrieval systems are data-driven and hard to explain, rendering them potentially unreliable due to limited training data and model complexity.

Reliability is crucial for many applications, such as self-driving and medical diagnosis. In addition to accurate predictions, it is important to be aware of any potential risks associated with the prediction. For example, rather than solely identifying the best-matching candidates from the diseases

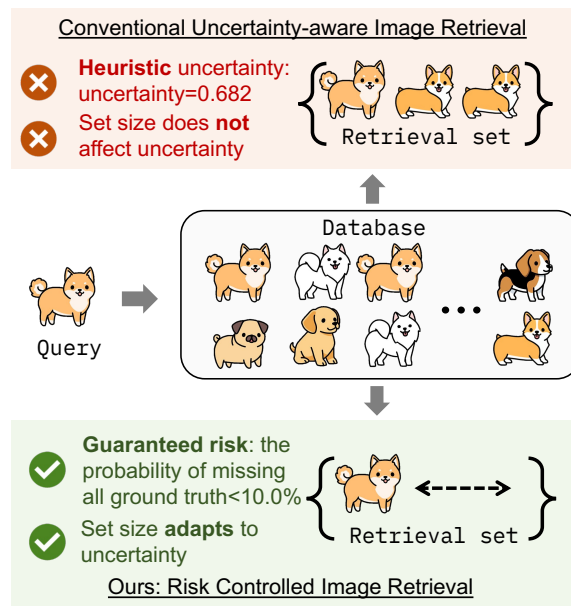


Figure 1: Illustration of RCIR and conventional uncertainty-aware image retrieval (e.g., (Warburg et al. 2021)): A conventional uncertainty-aware image retrieval provides a heuristic notion of uncertainty, and has a fixed retrieval set size however uncertain the query is. In contrast, RCIR provides a retrieval set that guarantees a predefined level of probability of covering a ground truth sample, and the retrieval size adapts to the uncertainty of the query sample.

databases, a medical practitioner would want a cluster of retrieval results with a specific level of reliability, say 90%, before making a diagnosis. Conventional image retrieval systems are inadequate for these tasks as they do not offer any measure of reliability.

To address this issue, researchers have developed the concept of uncertainty estimation for image retrieval. This involves estimating the level of uncertainty for both query and database samples. Approaches including (Warburg et al. 2021; Chang et al. 2020; Zhang, Wang, and Deng 2021) involves using high uncertainty as an indicator of potential prediction inaccuracies. This research partially addresses the

issue of uncertainty in image retrieval reliability. However, there are limitations to the uncertainty estimation approach. Firstly, the estimated uncertainty is merely a heuristic measure rather than a guarantee, leaving practitioners with only a vague idea of the prediction’s reliability. Secondly, the estimated uncertainties are independent of the retrieval set size, despite the fact that having more candidates increases the likelihood of covering the ground truth.

We propose a novel image retrieval framework called Risk Controlled Image Retrieval (RCIR) that addresses such limitations. RCIR generates adaptive retrieval sets conforming to a predefined level of risk¹ by introducing two modules, 1) adaptive retrieval and 2) risk control. The adaptive retrieval module employs a common uncertainty estimator to provide a heuristic uncertainty for the query and determine a prior retrieval set size. Then the risk control module adjusts the retrieval set size to comply with the predefined risk level and prior retrieval set size. We summarize the contributions of this paper as follows:

1. We propose an adaptive retrieval strategy that adapts retrieval size based on the commonly estimated heuristic uncertainty.
2. We for the first time enable an image retrieval system to generate retrieval sets that meet a predefined level of risk.
3. We demonstrate the effectiveness of the proposed methods by experimental results on four image retrieval datasets: the Stanford CAR-196 (Krause et al. 2013), CUB-200 (Wah et al. 2011), the Pittsburgh dataset (Torii et al. 2013) and the ChestX-Det dataset (Lian et al. 2021).

2 Related Work

2.1 Image Retrieval

Image retrieval involves building a tagged database offline and searching it online, where images are represented by feature vectors. Therefore, image retrieval’s effectiveness relies on the feature extractor’s representation power. Initially, hand-crafted image features such as SIFT (Lowe 1999) were primarily used. However, with the superior performance of deep learning-based features from pretrained CNNs (Babenko et al. 2014), hand-crafted features have become gradually obsolete. Recent research on image retrieval demonstrates that deep learning-based features can be effectively learned end-to-end with ranking loss functions (Hadsell, Chopra, and LeCun 2006; Schroff, Kalenichenko, and Philbin 2015; Sohn 2016). In this sense, image retrieval has evolved into a metric learning problem, with the aim of learning a mapping function that creates an embedding space where similar objects are positioned close together while dissimilar objects farther apart. Loss functions, including contrastive loss (Hadsell, Chopra, and LeCun 2006), triplet loss (Schroff, Kalenichenko, and Philbin 2015), N-pairs loss (Sohn 2016), etc., have been studied to enhance metric learning, which in turn benefits image retrieval.

¹The risk is defined as the probability of the retrieval set missing all ground truth samples of the query samples. Please see Sec.3.3 for a formal definition.

2.2 Uncertainty Estimation

Deep learning has achieved tremendous success in numerous computer vision tasks, but its black-box working mechanism has raised concerns about its reliability. Uncertainty estimation is a way to quantify the confidence of the model in its prediction. Uncertainty of predictions can arise from either the data’s inherent uncertainty or the model’s uncertainty, known as aleatoric and epistemic uncertainty, respectively (Kendall and Gal 2017). To quantify epistemic uncertainty, Variational Inference (VI)-based methods such as Monte Carlo (MC) Dropout are used to approximate Bayesian Neural Networks (BNNs), where the weights of the networks are modeled as distributions. Ensemble method (Fort, Hu, and Lakshminarayanan 2019) initiate multiple instances of a same model and then take the variances of predictions as an uncertainty level. On the other hand, researchers typically estimate aleatoric uncertainty by learning it via an additional head parallel to the network.

In image retrieval, DUL (Chang et al. 2020) learns aleatoric uncertainty by constructing a stochastic embedding space where the uncertainty is regularized by a KL divergence loss. BTL (Warburg et al. 2021) utilizes a bayesian loss function that enforces triplet constraints on stochastic embeddings. (Taha et al. 2019) shows MCD can be employed in image retrieval to quantify epistemic uncertainty. Current research on uncertainty estimation in image retrieval is primarily concerned with quantifying the likelihood of a pair of images being similar or dissimilar, albeit with only a heuristic notion of uncertainty. Our objective is to retrieve a set of images with a guarantee of containing the ground truth samples of a given query sample with a user-specified probability.

The framework of conformal prediction guarantees the correctness of a prediction (Vovk, Gammerman, and Shafer 2005). Conformal quantile regression (Romano, Patterson, and Candes 2019) enhances this approach to deliver prediction intervals with guaranteed accuracy. Building on this idea, DFUQ (Angelopoulos et al. 2022) proposes generating risk-guaranteed intervals in image regression, which has motivated us to tackle the constraints of existing image retrieval methods. However, it is important to note that DFUQ is specifically designed for regression tasks that rely on true labels. On the other hand, our image retrieval approach learns image embeddings without the use of true labels. Furthermore, the uncertainty estimation methods for regression tasks are distinct from those used in image retrieval since true labels are not available. These differences make it challenging to provide a risk-guaranteed retrieval set in image retrieval, highlighting the need for a shift in methodology.

3 Method

The RCIR framework extends image retrieval pipelines that incorporate heuristics for estimating uncertainty. In this section, we first explain the standard image retrieval pipeline. Next, we discuss three popular uncertainty estimation techniques for image retrieval. Lastly, we present the RCIR framework.

3.1 Image Retrieval

In an image retrieval pipeline, a feature extractor f_e is trained to map images from high-dimension image space to a low-dimension embedding space. In the embedding space, similar samples are close and dissimilar samples are far apart. Suppose there is a dataset $\{\mathcal{Q}, \mathcal{D}\}$, where \mathcal{Q} denotes query set and \mathcal{D} database. Given i^{th} query sample $X_i^{\mathcal{Q}} \in \mathcal{Q}$ (superscript denotes which set it belongs), its most similar samples $\{Y_{i,j} | j = 1, 2, \dots, K\}$ are retrieved from \mathcal{D} :

$$\{Y_{i,j} | j = 1, 2, \dots, K\} = \mathcal{R}_{[K, f_e]}(X_i^{\mathcal{Q}}), \quad (1)$$

where $\mathcal{R}_{[K, f_e]}$ represents a retrieval function conditioned on K and f_e :

$$\begin{aligned} \mathcal{R}_{[K, f_e]}(X_i^{\mathcal{Q}}) &= \{x | x \in \mathcal{P}, \mathcal{P} \subseteq \mathcal{D}, |\mathcal{P}| = K, \\ & d[f_e(X_i^{\mathcal{Q}}), f_e(x)] \leq d[f_e(X_i^{\mathcal{Q}}), f_e(y)], \\ & \forall y \in \mathcal{D} \setminus \mathcal{P}\} \end{aligned} \quad (2)$$

where d denotes a metric criterion, and K the number of the retrieved candidates, f_e the feature extractor.

The above image retrieval pipeline has been the de facto standard in the image retrieval community. However, it merely retrieves a set of best matching candidates, without any indicator showing how reliable the retrieval set is. This is problematic in risk-sensitive scenarios, where the reliability of the prediction is crucial.

3.2 Uncertainty-aware Image Retrieval

Uncertainty estimation mitigates this issue by estimating a heuristic notion of uncertainty for each query and database sample. Existing uncertainty-aware image retrieval methods include three methodologies: 1) estimate model uncertainty by Bayesian Neural Networks (Gal and Ghahramani 2016), 2) predict uncertainty by a deterministic model (Warburg et al. 2021), and 3) estimate uncertainty by an ensemble of models. We briefly introduce these methods in what follows.

Uncertainty Estimated by a BNN Bayesian approaches treat the weights of a neural network as distributions, instead of as deterministic values. However, obtaining the analytical posterior distribution for the weights is intractable due to the difficulty of acquiring evidence. Researchers have utilized various methods to address this challenge, with variational inference being the most widely employed. Monte Carlo Dropout (MCD) (Gal and Ghahramani 2016) initializes this methodology by assuming a mixed Gaussian distribution on each weight, which makes the sampling of weights equivalent to applying dropout operations. In our image retrieval setting, we apply dropout to all conventional layers of the feature extractor with a dropout rate p . Features μ and their heuristic uncertainties σ^2 are obtained by applying dropout at test time and feed forwarding T times:

$$\begin{aligned} \mu &= \frac{1}{T} \sum_{t=1}^T f_{e_t \sim \theta}(X), \\ \sigma^2 &= \frac{1}{T} \sum_{t=1}^T (f_{e_t \sim \theta}(X) - \mu)^2. \end{aligned} \quad (3)$$

where θ denotes the weights posterior distribution.

Uncertainty Estimated by an Ensemble Ensemble method (Fort, Hu, and Lakshminarayanan 2019) trains multiple instances of a same deterministic model, each with random initial weights. During inference time, predictions of all models are averaged, and the uncertainty is obtained as the variance of the predictions. Provided that there are N instances, the mean and variance of the predictions are:

$$\begin{aligned} \mu &= \frac{1}{N} \sum_{i=1}^N f_{e_i}(X), \\ \sigma^2 &= \frac{1}{N} \sum_{i=1}^N (f_{e_i}(X) - \mu)^2. \end{aligned} \quad (4)$$

Uncertainty Estimated by a Single Deterministic Model

Multiple feed forward propagations in MCD can cause overhead, and using multiple model instances can result in increased memory usage. In comparison, a single deterministic model is an attractive approach for estimating uncertainty. (Warburg et al. 2021) constructs a Gaussian distribution for each feature, i.e., $f_e(X) \sim \mathcal{N}(\mu, \sigma^2)$. A bayesian triplet loss is introduced to enforce triplet contrastive learning among these probabilistic features. The network is built upon a common image retrieval model by adding a variance head f_u parallel to the mean head f_e . Once trained, the model can output μ and σ^2 using only one feed forward propagation:

$$[\mu, \sigma^2] = [f_e(X), f_u(X)]. \quad (5)$$

In summary, uncertainties of features can be obtained through a BNN-based method, an ensemble, or a single deterministic model. Nevertheless, all of these methods only provide a *heuristic* notion of uncertainty (Angelopoulos et al. 2022), which is not a guarantee. That said, even with the estimated uncertainty, the retrieval set *cannot* be interpreted as a likelihood of encompassing the ground truth samples of a given query sample.

3.3 Risk Controlled Image Retrieval

The problems of existing uncertainty-aware image retrieval methods are problematic in two senses:

1. The heuristic notion of uncertainty cannot serve the purpose of a clear probability interpretation of the retrieval set.
2. The retrieval set's uncertainty is usually represented by the query sample's uncertainty (Warburg et al. 2021), which does not take into the retrieval set size into account. This means that for a given query sample, a retrieval set with 1 samples will be assigned the same uncertainty as a retrieval set with 10 samples. However, a larger retrieval set is obviously more likely to cover the ground truth than a smaller one.

We solve these two issues by proposing RCIR, which provides retrieval sets that guarantee to cover the ground truth samples with a predefined level of probability. And the retrieval set size is dynamically adapted to reflect the uncertainty of the query sample.

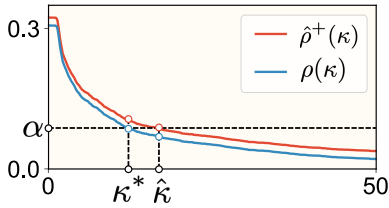


Figure 2: The $\rho - \kappa$ curve on the CAR-196 calibration set: the risk ρ is monotone nonincreasing with κ .

Risk Notion In RCIR, we denote the risk of a image retrieval system by ρ , which is defined as the probability of a retrieval set missing all ground truth samples of the given query sample:

$$\rho(\mathcal{R}) = \mathbb{E}_{X \in \mathcal{Q}}[\ell(\mathcal{R}(X), \mathcal{S}(X))], \quad (6)$$

where \mathcal{R} denotes a generic retrieval system as in (2), \mathcal{S} denotes retrieving all ground truth samples, and ℓ indicates if the retrieval set misses all ground truth samples:

$$\ell(\mathcal{R}(X), \mathcal{S}(X)) = \mathbb{1}(\mathcal{R}(X) \cap \mathcal{S}(X) = \emptyset). \quad (7)$$

The risk function $\rho(\cdot)$ evaluates the performance of a retrieval system \mathcal{R} , and is bounded between 0 and 1: $\rho(\mathcal{R}) = 0$ occurs when the retrieval set $\mathcal{R}(X)$ always covers at least one ground truth, and $\rho(\mathcal{R}) = 1$ happens when the retrieval set $\mathcal{R}(X)$ never covers a ground truth.

Adaptive Retrieval In practice, practioners may want ‘easy’ query samples to have smaller retrievals set than those of ‘hard’ query samples, because this would save downstream processing time on easy ones without sacrificing accuracy. Therefore, we propose to adapt the retrieval set size based on the query’s difficulty level. And we employ the common heuristic uncertainty of query samples as a coarse measure of difficulty. Specifically, we propose a simple yet effective mapping function $\pi_\kappa(\cdot)$ as follows:

$$\pi_\kappa : K_i \leftarrow \lceil \kappa \cdot \Phi[f_u(X_i^{\mathcal{Q}})] \rceil, \quad (8)$$

where $\kappa \in \mathbb{R}^+$ denotes a non-negative real number, f_u is a heuristic uncertainty estimator, Φ means normalizing the result to $[0, 1]$, and $\lceil \cdot \rceil$ means rounding up to the nearest integer. The mapping function is essential as it allows RCIR to retrieve varying numbers of candidates, tailored to the uncertainty of each query sample. Compared to the conventional retrieval function in (1) that always returns a fixed number (i.e., K) of candidates, our adaptive retrieval function retrieves K_i candidates depending on the choice of κ and the uncertainty of the query sample:

$$\{Y_{i,j} | j = 1, 2, \dots, K_i\} = \mathcal{R}_{[\kappa, f_u, f_e]}(X_i^{\mathcal{Q}}) \quad (9)$$

Risk Control The adaptive retrieval strategy makes the retrieval set varying according to the uncertainty of the query samples, but it still cannot ensure the risk of retrieval set is below any predefined level. In this section, we will discuss how to make risk of the adaptive retrieval set controllable.

Lemma 3.1. *Given a dataset $\{\mathcal{Q}, \mathcal{D}\}$, let the pretrained feature extractor f_e and uncertainty estimator f_u be fixed, then the risk function $\rho(\mathcal{R}_{[\kappa, f_u, f_e]})$ is a monotone nonincreasing function of the κ for $\forall \kappa \in \mathbb{R}^+$.*

Algorithm 1: Compute $\hat{\kappa}$.

Input: Calibration set $\{\mathcal{Q}, \mathcal{D}\}$, risk level α , error rate δ , trained feature extractor f_e , trained heuristic uncertainty estimator f_u .

Output: Parameter $\hat{\kappa}$.

```

1:  $\kappa \leftarrow 1, \hat{\rho}^+(\kappa) \leftarrow 1$ 
2: while  $\hat{\rho}^+(\kappa) > \alpha$  do
3:    $\kappa = \kappa + \Delta\kappa$ 
4:   for  $i$  in  $1, 2, \dots, |\mathcal{Q}|$  do
5:      $\ell_i = \mathbb{1}[\mathcal{R}_{[\kappa, f_u, f_e]}(X_i^{\mathcal{Q}}) \cap \mathcal{S}(X_i^{\mathcal{Q}}) = \emptyset]$ 
6:   end for
7:    $\hat{\rho}(\kappa) = \frac{1}{|\mathcal{Q}|} \sum_i \ell_i$ 
8:    $\hat{\rho}^+(\kappa) = \hat{\rho}(\kappa) + \sqrt{\frac{1}{2n} \log \frac{1}{\delta}}$ 
9: end while
10:  $\hat{\kappa} = \kappa - \Delta\kappa$ 
11: return  $\hat{\kappa}$ 

```

Proof. For any i^{th} query $X_i^{\mathcal{Q}}$, if $\kappa_1 > \kappa_2$, then $K_{i, \kappa_1} \geq K_{i, \kappa_2}$ (by mapping function (8) as f_u is fixed), which means $|\mathcal{R}_{[\kappa_1, f_u, f_e]}(X_i^{\mathcal{Q}})| \geq |\mathcal{R}_{[\kappa_2, f_u, f_e]}(X_i^{\mathcal{Q}})|$.

Since in a retrieval system the candidates are retrieved based on a consistent distance metric d (see (2)),

$$\mathcal{R}_{[\kappa_2, f_u, f_e]}(X_i^{\mathcal{Q}}) \subseteq \mathcal{R}_{[\kappa_1, f_u, f_e]}(X_i^{\mathcal{Q}}),$$

then, by the loss definition in (7),

$$\ell(\mathcal{R}_{[\kappa_2, f_u, f_e]}(X_i^{\mathcal{Q}}), \mathcal{S}(X_i^{\mathcal{Q}})) \geq \ell(\mathcal{R}_{[\kappa_1, f_u, f_e]}(X_i^{\mathcal{Q}}), \mathcal{S}(X_i^{\mathcal{Q}})),$$

and thus,

$$\rho(\mathcal{R}_{[\kappa_2, f_u, f_e]}) \geq \rho(\mathcal{R}_{[\kappa_1, f_u, f_e]}).$$

□

For a trained image retrieval system, the f_u, f_e are fixed, therefore, the risk of the adaptive retrieval system depends on the parameter κ , which we denote as $\rho(\kappa)$.

Theorem 3.2. *Assume $\rho(\kappa)$ is a monotone nonincreasing function, and an upper confidence bound $\hat{\rho}^+(\kappa)$ for each κ is accessible. If $\forall \kappa \in \mathbb{R}^+$,*

$$P(\rho(\kappa) \leq \hat{\rho}^+(\kappa)) \geq 1 - \delta. \quad (10)$$

let $\hat{\kappa}$ denotes the smallest κ such that for any $\kappa > \hat{\kappa}$ we have $\hat{\rho}^+(\kappa) \leq \alpha$:

$$\hat{\kappa} = \inf\{\kappa : \hat{\rho}^+(\kappa') < \alpha, \forall \kappa' > \kappa\}. \quad (11)$$

then

$$P(\rho(\hat{\kappa}) \leq \alpha) \geq 1 - \delta. \quad (12)$$

Proof. Consider the smallest κ that controls the risk to be less than α , i.e.,

$$\kappa^* = \inf\{\kappa : \rho(\kappa) \leq \alpha\}, \quad (13)$$

Suppose $\rho(\hat{\kappa}) > \alpha$, then by the monotonicity of $\rho(\kappa)$, we have $\hat{\kappa} < \kappa^*$. Eq.(11) implies $\hat{\rho}^+(\kappa^*) < \alpha$, and Eq.(13) implies $\rho(\kappa^*) = \alpha$ (by continuity of $\rho(\kappa)$). According to (10), this case only happens with a probability of at most δ . Therefore, $P(\rho(\hat{\kappa}) \leq \alpha) \geq 1 - \delta$. Fig.2 provides an experimental example that helps to visualize the proof process. □

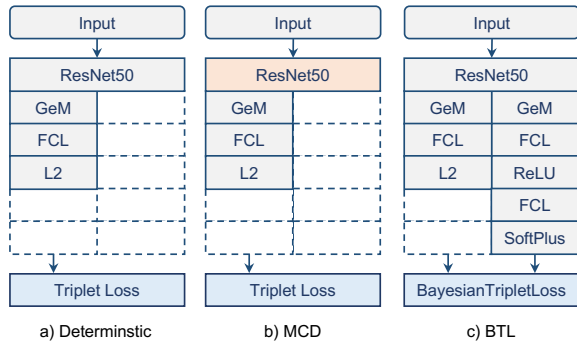


Figure 3: The network architectures of different methods.

With Eq.(11), we can proceed to determine an upper confidence bound, denoted by $\hat{\rho}^+(\kappa)$. According to (Bates et al. 2021), Hoeffding’s Inequality is applicable to our risk function $\rho(\kappa)$, which is bounded by one. We denote the empirical risk on the calibration set by $\hat{\rho}(\kappa)$. Hoeffding’s Inequality indicates that

$$P(\hat{\rho}(\kappa) - \rho(\kappa) \leq -x) \leq e^{-2nx^2}, \quad (14)$$

which implies an upper confidence bound

$$\hat{\rho}^+(\kappa) = \hat{\rho}(\kappa) + \sqrt{\frac{1}{2n} \log\left(\frac{1}{\delta}\right)}. \quad (15)$$

Given a predefined risk requirement, i.e., risk level α and error rate δ , we use (11) to compute $\hat{\kappa}$. The computation process is outlined in Algorithm 1. Once we have $\hat{\kappa}$, we can ensure that the retrieval set will cover the ground truth samples with a probability of $1 - \alpha$ and limit the error rate to δ .

4 Experiments

4.1 Datasets

CUB-200 (Wah et al. 2011) contains 11,788 images of 200 classes. Each class has at least 50 images. We use the first 100 classes as a training set and the other 100 as a test set.

Stanford CAR-196 Stanford CAR-196 (Krause et al. 2013) contains 16,185 images of 196 classes. Each class has at least 80 images. We use the first 98 classes as the training set and the other 98 classes as test set.

Pittsburgh (Torii et al. 2013) is a large image database from Google Street View. Following the split of NetVLAD (Arandjelovic et al. 2016), we adopt the subset that consists of 10k samples in the training/validation/test split.

ChestX-Det (Lian et al. 2021) is a subset of the public dataset NIH ChestX-ray14, and it contains 3543 images with 14 classes (13 categories of diseases and normal cases). We choose samples of the six classes as training set, and the rest as the test set.

For all datasets, we randomly choose 50% images from the test set to form the calibration set.

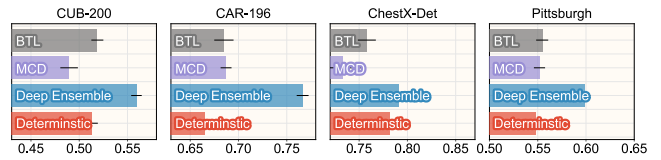


Figure 4: The Recall@1 results of different methods on different test sets. The error bars represent the standard deviation of the results of 10 trials.

4.2 Implementations

Our proposed RCIR is versatile and can be applied to any image retrieval model that provides heuristic uncertainty. For comparison purposes, we use the image retrieval model from (Warburg et al. 2021) as the backbone model. Based on this backbone, we build four comparing methods: **Deterministic**, **MCD**, **BTL** and **Deep Ensemble**. The architectures of the first three are depicted in Fig.3. The Deterministic model is composed of ResNet-50 (He et al. 2016) backbone, a GeM layer (Radenović, Tolias, and Chum 2018), a fully connected layer and a L2-normalization layer. The Deterministic model is trained with the triplet loss (Schroff, Kalenichenko, and Philbin 2015). The MCD model is same as the Deterministic except that we apply dropout to all conventional layers of the backbone during both training and testing time. The BTL model has an additional variance head, and it is trained with the bayesian triplet loss (Warburg et al. 2021). We build 5 deterministic models to form the Deep Ensemble model.

We train the above models using the Adam optimizer, with an initial learning rate of 10^{-5} and an exponential learning rate scheduler with gamma 0.99. The weight decay is set to 10^{-3} . Our model’s feature dimension is 2048, and the variance dimension is 1. We adopt a hard mining strategy and feed the model with triplets that violate the triplet margin (Warburg et al. 2021) (please see supplementary for details).

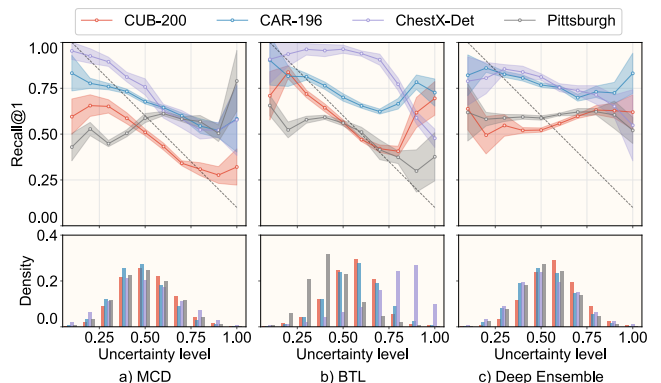


Figure 5: The reliability diagrams of different methods on different datasets. The colored shadows represent the standard deviation of the results of 10 trials.

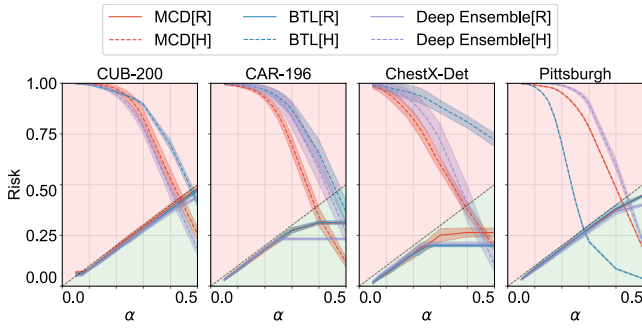


Figure 6: The risks on different datasets: risk is well controlled by RCIR (see $\times[R]$) under different risk level α (with an error rate $\delta = 0.1$). The colored shadows represent the standard deviation of the results of 10 trials.

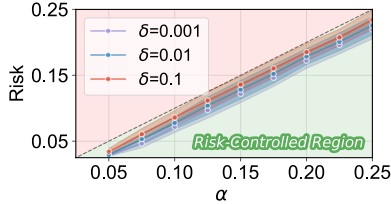


Figure 7: The risks on the Pittsburgh datasets with different error rate δ (by BTL[R]): smaller δ will lead to more conservative retrievals (e.g., larger retrieval size). The colored shadows represent the standard deviation of the results of 10 trials.

4.3 Metrics

Empirical risk The goal of the proposed RCIR is to control the empirical risk. The empirical risk is evaluated on the test split, and should be below than α with a probability of $1 - \delta$ (according to Theorem.3.2).

Retrieval size It is possible that the risk control algorithm resorts to large retrieval sets to lower the empirical risk. However, large retrieval sets tend to include more negative samples and can be inefficient for downstream processing. Ideally, the retrieval size should be minimized while still controlling the risk to stay below the threshold.

Recall@K The performance of the retrieval model itself matters. We use Recall@K as the metric, which is defined as the percentage queries whose top-K retrieved samples have at least one sample that share the same class as the query.

ECE@1 Expected Calibrated Error (ECE) (Warburg et al. 2021) is used to measure the quality of the estimated heuristic uncertainty. We follow (Warburg et al. 2021) and adopt ECE@1, where a lower value indicates a better-calibrated uncertainty.

Qualitative visualization We also provide qualitative visualizations of the image retrieval results.

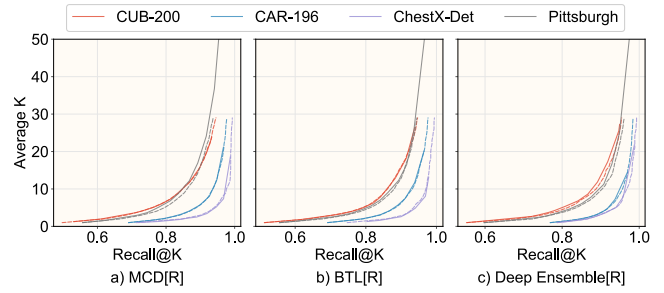


Figure 8: The average K across different methods on different test sets (*solid line* — means using the proposed adaptive retrieval, while *dashed line* - - - the traditional fixed retrieval size): When achieving the same recall, the adaptive strategy and fixed strategy have a similar average retrieval set size. This indicates that the adaptive strategy does not rely on brute-forcelly increasing K to control the risk.

4.4 Results

Image retrieval performance We begin by evaluating the retrieval performance of various methods. The Recall@1 results of different methods on various test sets are presented in Fig.4. BTL achieves a higher recall@1 than Deterministic on most datasets, suggesting that an appropriate uncertainty-aware image retrieval can enhance image retrieval performance. Nevertheless, MCD’s performance is inconsistent when compared to Deterministic, which may be due to the impact of the dropout layers on the representation power, depending on the dataset. Deep Ensemble achieves the best performance, which can be attributed to the fact that it utilizes multiple models to average out noises.

Uncertainty estimation performance Fig.5 depicts the reliability diagrams of different methods across the four datasets. It can be seen that none of these curves conforms to the ideally-calibrated line (dashed line), indicating that the heuristic uncertainty itself is not reliable. Moreover, the gaps between the curves and the dashed line vary across datasets for both MCD, BTL and Deep Ensemble, implying that the same uncertainty estimation method cannot consistently perform across different datasets.

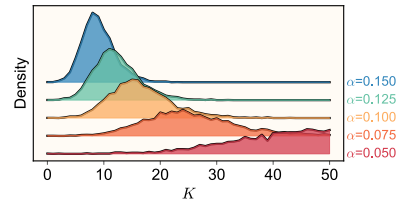


Figure 9: The retrieval size, K , on the Pittsburgh test set (by BTL[R]): retrieval set size adapts to the risk level α .

Risk control performance We incorporate RCIR into MCD, BTL, and Deep Ensemble, resulting in the image retrieval pipelines MCD[R], BTL[R], and Deep Ensemble[R], respectively. Meanwhile, to evaluate the practical usefulness of heuristic uncertainty, we normalize heuristic uncertainties

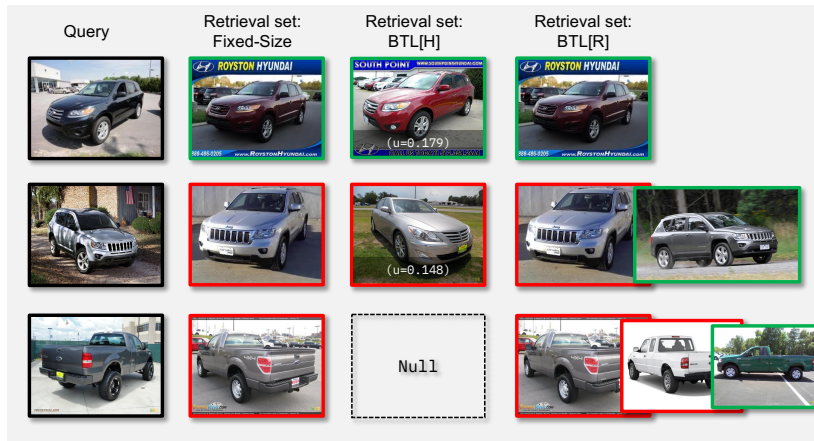


Figure 10: The qualitative visualization of retrievals on CAR-196 dataset by different methods (Red border denotes a wrong candidate, while Green correct): with a predefined risk level $\alpha = 0.2$ and error rate $\delta = 0.1$, BTL[R] adjusts the size of retrievals to select the uncertainty while ensuring coverage.

to the range $[0, 1]$ based on their statistics on the calibration set. Then each query-candidate pair’s uncertainty is calculated as the sum of their individual uncertainties (Warburg et al. 2021). This will result in three comparing methods: MCD[H], BTL[H] and Deep Ensemble[H]. With a predefined a risk level α and error rate δ , MCD[R], BTL[R] and Deep Ensemble[R] calculate $\hat{\kappa}$ using Algorithm.1 on the calibration set. For fairness, MCD[H], BTL[H] and Deep Ensemble[H] retrieve as many candidates as \times [R] can achieve, then only keep the pairs whose uncertainties are below α . We perform the image retrieval on the test sets and report their empirical risks.

Fig.6 shows the empirical risk of different methods on different datasets. It can be observed that the risks of \times [R] are always below the predefined risk levels α . This means that even before retrieval we can say for sure that the retrievals of \times [R] has a α probability of covering the ground truth, with only a δ probability of being wrong. In comparison, heuristic uncertainty-only method, including MCD[H], BTL[H] and Deep Ensemble[H], exhibit risks higher than the predefined risk levels in the range $\alpha < 0.4$. The results show that the heuristic uncertainty alone is not reliable to be used for risk control, and RCIR can control the risk well..

In addition, we show the effect of using different δ , which controls how conservative the RCIR is. Fig.7 shows the empirical risk with different δ on the Pittsburgh dataset. With a smaller δ , RCIR would be more conservative (i.e., larger retrieval size) to ensure the risk is below the given α .

It is possible that RCIR always resort to large retrieval sets to lower the empirical risk, in which situation the risk is trivially controlled but the retrieval sets would be of less practical use. To examine this, we compare MCD[R], BTL[R] and Deep Ensemble[R] against their fix-size retrieval counterparts. Fig.8 shows that when achieving the same recall@ K , \times [R] and their fix-size retrieval counterparts have a similar average retrieval set size. This indicates that \times [R] does not rely on brute-forcelly increasing K to control the risk. However, we also notice that MCD[R] and Deep Ensemble[R] on

the Pittsburgh test set has a slightly larger average retrieval set size than their fix-size retrieval counterparts, This is likely due to poor uncertainty estimation on Pittsburgh, as shown in Fig.5.

Qualitative visualization The distribution of retrieval size on the Pittsburgh test set is presented in Fig. 9. It is evident that the retrieval size varies with the risk level α : a smaller α results in a larger retrieval size, and vice versa. This helps practitioners save time on easy queries and focus on more difficult ones. Fig.10 shows the qualitative visualization of retrievals on the CAR-196 dataset by different methods. In the first row, it is evident that when a relatively easy query is provided, all methods successfully retrieve the correct results. Moving on to the second row, where the query is more challenging, the fixed-size retrieval method fails without any indication, and BTL[H] fails as well with a low heuristic number. However, BTL[R] takes into account the difficulty of the query and retrieves an additional candidate, resulting in the correct answer. As for the third row, it represents a more demanding query. BTL[H] generates no candidate in this case, while BTL[R] retrieves more candidates to meet the coverage requirement.

5 Conclusion

This paper introduces RCIR, a significant improvement to the current uncertainty estimation for image retrieval. Unlike the heuristic notion of uncertainty provided by existing methods, RCIR offers a risk guarantee. This paper includes a theoretical analysis of the risk bound of RCIR and presents extensive experimental results that demonstrate its efficacy in controlling the risk of a generic image retrieval system. We believe that the advancement provided by RCIR can benefit risk-sensitive applications, such as medical image retrieval and autonomous driving.

References

- Angelopoulos, A. N.; Kohli, A. P.; Bates, S.; Jordan, M.; Malik, J.; Alshaabi, T.; Upadhyayula, S.; and Romano, Y. 2022. Image-to-image regression with distribution-free uncertainty quantification and applications in imaging. In *International Conference on Machine Learning*, 717–730. PMLR.
- Arandjelovic, R.; Gronat, P.; Torii, A.; Pajdla, T.; and Sivic, J. 2016. NetVLAD: CNN architecture for weakly supervised place recognition. In *Proceedings of the IEEE conference on computer vision and pattern recognition*, 5297–5307.
- Babenko, A.; Slesarev, A.; Chigorin, A.; and Lempitsky, V. 2014. Neural codes for image retrieval. In *Computer Vision—ECCV 2014: 13th European Conference, Zurich, Switzerland, September 6–12, 2014, Proceedings, Part I 13*, 584–599. Springer.
- Bates, S.; Angelopoulos, A.; Lei, L.; Malik, J.; and Jordan, M. 2021. Distribution-free, risk-controlling prediction sets. *Journal of the ACM (JACM)*, 68(6): 1–34.
- Chang, J.; Lan, Z.; Cheng, C.; and Wei, Y. 2020. Data uncertainty learning in face recognition. In *Proceedings of the IEEE/CVF conference on computer vision and pattern recognition*, 5710–5719.
- Cheng, Y.; and Wang, H. 2019. A modified contrastive loss method for face recognition. *Pattern Recognition Letters*, 125: 785–790.
- Fort, S.; Hu, H.; and Lakshminarayanan, B. 2019. Deep ensembles: A loss landscape perspective. *arXiv preprint arXiv:1912.02757*.
- Gal, Y.; and Ghahramani, Z. 2016. Dropout as a bayesian approximation: Representing model uncertainty in deep learning. In *international conference on machine learning*, 1050–1059. PMLR.
- Hadsell, R.; Chopra, S.; and LeCun, Y. 2006. Dimensionality reduction by learning an invariant mapping. In *2006 IEEE Computer Society Conference on Computer Vision and Pattern Recognition (CVPR'06)*, volume 2, 1735–1742. IEEE.
- He, K.; Zhang, X.; Ren, S.; and Sun, J. 2016. Deep residual learning for image recognition. In *Proceedings of the IEEE conference on computer vision and pattern recognition*, 770–778.
- Kendall, A.; and Gal, Y. 2017. What uncertainties do we need in bayesian deep learning for computer vision? *Advances in neural information processing systems*, 30.
- Krause, J.; Stark, M.; Deng, J.; and Fei-Fei, L. 2013. 3d object representations for fine-grained categorization. In *Proceedings of the IEEE international conference on computer vision workshops*, 554–561.
- Lian, J.; Liu, J.; Zhang, S.; Gao, K.; Liu, X.; Zhang, D.; and Yu, Y. 2021. A structure-aware relation network for thoracic diseases detection and segmentation. *IEEE Transactions on Medical Imaging*, 40(8): 2042–2052.
- Lowe, D. G. 1999. Object recognition from local scale-invariant features. In *Proceedings of the seventh IEEE international conference on computer vision*, volume 2, 1150–1157. Ieee.
- Radenović, F.; Toliás, G.; and Chum, O. 2018. Fine-tuning CNN image retrieval with no human annotation. *IEEE transactions on pattern analysis and machine intelligence*, 41(7): 1655–1668.
- Romano, Y.; Patterson, E.; and Candes, E. 2019. Conformalized quantile regression. *Advances in neural information processing systems*, 32.
- Schroff, F.; Kalenichenko, D.; and Philbin, J. 2015. Facenet: A unified embedding for face recognition and clustering. In *Proceedings of the IEEE conference on computer vision and pattern recognition*, 815–823.
- Sohn, K. 2016. Improved deep metric learning with multi-class n-pair loss objective. *Advances in neural information processing systems*, 29.
- Taha, A.; Chen, Y.-T.; Yang, X.; Misu, T.; and Davis, L. 2019. Exploring uncertainty in conditional multi-modal retrieval systems. *arXiv preprint arXiv:1901.07702*.
- Torii, A.; Sivic, J.; Pajdla, T.; and Okutomi, M. 2013. Visual place recognition with repetitive structures. In *Proceedings of the IEEE conference on computer vision and pattern recognition*, 883–890.
- Vovk, V.; Gammerman, A.; and Shafer, G. 2005. *Algorithmic learning in a random world*, volume 29. Springer.
- Wah, C.; Branson, S.; Welinder, P.; Perona, P.; and Belongie, S. 2011. The caltech-ucsd birds-200-2011 dataset.
- Warburg, F.; Jørgensen, M.; Civera, J.; and Hauberg, S. 2021. Bayesian triplet loss: Uncertainty quantification in image retrieval. In *Proceedings of the IEEE/CVF International conference on Computer Vision*, 12158–12168.
- Yao, H.; Zhang, S.; Hong, R.; Zhang, Y.; Xu, C.; and Tian, Q. 2019. Deep representation learning with part loss for person re-identification. *IEEE Transactions on Image Processing*, 28(6): 2860–2871.
- Zhang, Y.; Wang, C.; and Deng, W. 2021. Relative uncertainty learning for facial expression recognition. *Advances in Neural Information Processing Systems*, 34: 17616–17627.